Available online at www.sciencedirect.com
SCIENCE DIRECT
Journal of Catalysis 232 (2005) 411–423
JOURNAL OF CATALYSIS
www.elsevier.com/locate/jcat

Effects of Brønsted acidity in the mechanism of selective oxidation of propane to acetone on CaY zeolite at room temperature

Jiang Xu, Barbara L. Mojet *, Jan G. van Ommen, Leon Lefferts

Catalytic Processes and Materials, Faculty of Science and Technology, Institute of Mechanics Processes and Control Twente (IMPACT), University of Twente, PO Box 217, 7500 AE, Enschede, The Netherlands

Received 9 December 2004; revised 21 March 2005; accepted 6 April 2005

Available online 10 May 2005

Abstract

The importance of Brønsted acid sites for partial oxidation of propane to acetone in CaY was investigated by in situ FTIR spectroscopy. With an increasing number of protons in Ca-Y, Volcano plots were observed for (1) amount of adsorbed propane; (2) initial acetone formation rate; (3) total amount of acetone after 20 h of reaction; (4) acetone selectivity. The results clearly show that Brønsted acidity increases the isopropylhydroperoxide (IHP) formation rate, most likely via a catalytic H^+ transfer, and IHP decomposition into acetone and water. Moreover, with increasing IHP concentration 2-propanol was found in addition to acetone. Since an increasing number of Brønsted acid sites implies a decreasing number of Ca^{2+} in the zeolite, an optimal H^+/Ca^{2+} ratio was observed for both activity and selectivity for acetone.

Keywords: CaY zeolite; Propane selective oxidation; Brønsted acidity; Acetone; Isopropylhydroperoxide

1. Introduction

Direct selective oxidation of light alkanes into valuable products is one of the most challenging subjects in catalytic chemistry, because of the global abundance of low alkanes and the huge economic incentives [1]. The main disadvantage of partial oxidation is that light alkanes are usually less reactive than the desired products, and further oxidation to CO_x is thermodynamically favored. Recent efforts at improvement of the selectivity of light alkane oxidation have mainly been based on catalysis over metals, metal oxides [1–3], or zeolite-supported metal oxides [4,5]. Although selectivity is much improved, all of these methods still generate substantial amounts of carbon oxides or other carbon fragmentation products, some even at low hydrocarbon conversion.

The inefficiency associated with low conversion has motivated the search for solid catalysts that are active and selective for the oxidation of light alkanes. Recently, a new approach of selective oxidation of alkanes (ethane, propane, isobutene, and cyclohexane) [6–10] on cation-exchanged Y zeolite was presented under photo or thermal conditions. The concept is that hydrocarbon and oxygen are confined in a restricted environment (zeolite cages), followed by the formation of charge transfer complex $[(CnH_{2n+2})^+O_2^-]$. The complex stabilizes in the presence of a strong electrostatic field due to cations. Alkyl hydroperoxide was observed as reaction intermediate. Complete selectivity was reported at conversions as high as 22%, by in situ FTIR measurements of propane oxidation to acetone for BaY zeolite. However, the catalytic reaction cycle was not yet closed, since no product desorption could be observed under these conditions. Based on the cation dependence, reaction activity was reported to increase in the order NaY < BaY < SrY < CaY with increasing cationic electrostatic field for the gas-phase reaction of cyclohexane to cyclohexanone [6,11] and propane to acetone [10]. Larsen et al. indicated that proton abstraction from the hydrocarbon radical cation to O_2^- is the rate-determining step for the conversion of cyclohexane

* Corresponding author. Fax: +31 53 4894683.
E-mail address: b.l.mojet@utwente.nl (B.L. Mojet).

0021-9517/$ – see front matter
doi:10.1016/j.jcat.2005.04.004

to cyclohexanone on BaY and NaY zeolites, because of the observation of a pronounced deuterium kinetic isotope effect [7].

Recent results from our group have shown that the rate of propane oxidation to acetone is influenced by the type of earth-alkali cations, zeolite Brønsted acidity, and cation position in the zeolite [10,12,13]. Cations in the supercage of zeolite Y are exclusively responsible for the propane oxidation reaction. A two-step mechanism with two different active sites was proposed: conversion of propane into isopropylhydroperoxide (IHP) takes place on earth-alkali cations, whereas the decomposition into acetone and water occurs by Brønsted acid sites, as follows:

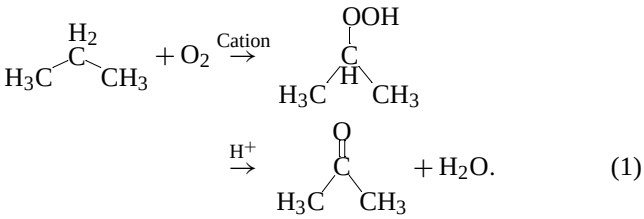

(1)

However, a systematic variation of the concentration of Brønsted acid sites is needed to investigate the relationship between Brønsted acidity and IHP conversion. Moreover, it is not yet clear whether the cation and Brønsted acid sites act independently in this reaction or a cooperation of both sites is needed. Furthermore, increased Brønsted acidity produced by the introduction of NH_4^+, followed by decomposition in cation-exchanged Y zeolite, will lead to a decrease in the electrostatic field of cations, because the total amount of positive charge (Brønsted acid or cation) that compensates for the negative zeolite framework should be the same. In other words, the cation and Brønsted acid sites cannot be varied independently.

Loss of product selectivity has been observed with increasing Brønsted acidity as a result of photooxidation of 1-alkenes, toluene, and *p*-xylene in cation-exchanged zeolites, leading to polymerization and condensation reactions [14,15]. Furthermore, in liquid-phase oxidation of cyclohexane on alkali or alkaline-earth exchanged Y zeolite, it has been shown that the Brønsted acidity acts as an inhibitor rather than as a catalyst [16]. In liquid phase, the typical radical reaction path via homolytic peroxide decomposition has been proposed. Although the restricted environment (zeolite cage) limits the diffusion of free radical to follow the chain propagation at low-temperature gas-phase reaction, nevertheless, a contribution of free-radical chemistry cannot be excluded.

To answer the above-mentioned questions, we investigated the details of propane selective oxidation reaction on a series of CaY zeolites with varying proton concentrations with the use of infrared spectrometry. The goal was to obtain insight into the effect of Ca^{2+} and acid sites on the reaction mechanism of selective propane oxidation.

2. Experimental

2.1. Materials

The base material used for this study was a NaY (Akzo Nobel; sample code 1122-207) with a Si/Al ratio of 2.5. The CaY zeolite was prepared by repeated aqueous exchange of the base NaY zeolite with 0.05 M calcium nitrate solutions repeated three times, followed by washing three times with distilled water; filtered; and dried at 100 °C overnight.

The series of HCaY zeolites were prepared by exchange of CaY zeolite with NH_4NO_3 solutions. The NH_4^+ loading of the zeolite was controlled by the concentration of NH_4^+ in the aqueous solution. All zeolites were prepared with the same procedure of washing and drying as described above. The final HCaY zeolites were obtained by decomposition at 500 °C under vacuum. After decomposition, Brønsted acid sites can be contributed by both decomposition of NH_4^+ ions and hydrolysis of water at Ca^{2+} sites. The chemical composition of catalysts (determined by X-ray fluorescence, XRF), Ca^{2+}/Al and NH_4^+/Al ratios, and sample names are listed in Table 1. The results show that Ca^{2+} was gradually replaced by NH_4^+, whereas the sodium content, which remains in CaY zeolite, decreased only slightly and remained almost constant for the series of HCaY zeolites.

Nevertheless, the NH_4^+ and Ca^{2+} cations cannot be varied independently, because the total amount of positive charge should remain constant. Thus, another two samples

Table 1
Chemical analysis of zeolite samples used in this study (as determined by XRF)

Zeolite	Chemical composition (wt%)[a]				Molar ratio		
	Al_2O_3	SiO_2	Na_2O	CaO	Na^+/Al	Ca^{2+}/Al	NH_4^+/Al[b]
Na–CaY71	21.8	66.0	3.67	8.59	0.28	0.36	–
Ca–NaY73	21.8	66.2	3.44	8.56	0.26	0.36	–
CaY	21.9	65.8	1.30	10.9	0.10	0.45	–
H(4)CaY	21.9	65.5	1.09	10.5	0.08	0.44	0.04
H(7)CaY	22.0	66.5	1.26	10.2	0.09	0.42	0.07
H(13)CaY	22.2	67.1	1.21	9.51	0.09	0.39	0.13
H(26)CaY	22.6	68.1	1.03	8.27	0.08	0.33	0.26

[a] Standard deviation is ±1% (relative error).
[b] NH_4^+ content was calculated based on the charge balance; iron content < 0.02 wt%.

were prepared to vary the concentration of Brønsted acid sites, while the calcium content was kept constant. A partial sodium back-exchanged CaY zeolite was prepared by ion exchanging CaY with a $NaNO_3$ solution, to remove the protons formed by the hydrolysis of calcium complex (sample designated as Na–CaY71). During back-exchange, it inevitably exchanges part of the calcium cation as well. Thus, a partially exchanged CaNaY was prepared with NaY and a controlled concentration of calcium nitrate solution (sample designated as Ca–NaY73), to make two catalysts with identical calcium contents and different Brønsted acid sites. After ion exchange, both samples were washed and dried according to the procedure described above. The catalyst chemical composition (determined by XRF) listed in Table 1 shows that the same Ca^{2+}/Al ratio was obtained. However, a higher Na^+/Al ratio for Na–CaY71 than for Ca–NaY73 was found. In addition, ^{27}Al MAS NMR showed no extra-framework aluminum for the studied samples, even not after activation at 500 °C.

2.2. Infrared spectroscopy studies

The zeolite powder (30 mg) was pressed into a self-supported wafer and analyzed in situ during adsorption and reaction by transmission FTIR spectroscopy with a Bruker Vector22 FTIR spectrometer with a MCT detector. A miniature cell, equipped with transparent CaF_2 windows, which can be evacuated to pressures below 10^{-7} mbar, was used for the in situ experiments. The temperature was variable from room temperature to 500 °C. Each spectrum consisted of 32 scans taken at 4 cm^{-1} resolution.

Zeolite samples were activated at 500 °C (ramp 10 °C/min) for 2 h in vacuum ($< 10^{-7}$ mbar) and subsequently cooled to 100 °C for ammonia adsorption. Ammonia was introduced into the infrared cell until equilibrium was reached at 1 mbar. Then the system was evacuated and spectra were recorded. The FTIR spectra for activated zeolite structure and ammonia adsorption were corrected for absorption by the background spectrum.

For propane-selective oxidation study, samples were activated in vacuum ($< 10^{-7}$ mbar) at 500 °C (ramp 10 °C/min) for 2 h, subsequently cooled to 200 °C (dwell 10 h), and cooled to room temperature. Loading of reactants (propane and oxygen) was controlled by gas pressure. Propane was introduced into the IR cell until equilibrium was reached at 1 mbar in the gas phase, followed by the addition of 40 mbar of oxygen. Calibration curves were made by adsorption of known amounts of acetone and 2-propanol at room temperature to determine the quantity of produced acetone from propane and oxygen. The amount of produced isopropylhydroxide (IHP) was determined by the increase in acetone quantity as a result of thermal conversion of IHP into acetone and water. The FTIR spectra in propane adsorption and reaction studies were corrected for absorption by the activated zeolite.

2.3. Ammonia temperature-programmed desorption studies

A home-made temperature-programmed desorption (TPD) setup connected to a UHV chamber with a mass spectrometer (Balzers QMG 420) was used for the desorption experiments. After activation at 10^{-3} mbar and 500 °C for 2 h, 60 mg of CaNaY zeolite samples was exposed to 10 mbar of ammonia at 100 °C (to avoid the physisorbed NH_3). When adsorption–desorption equilibrium was reached, the sample was evacuated for 1.5 h at 10^{-3} mbar. Then TPD, with an increment of 10 °C/min up to 700 °C, was started.

3. Results and discussion

3.1. Catalyst characterization

Calibrated transmission FTIR spectra of the activated CaY and series HCaY zeolites samples are given in Fig. 1a. All samples showed an isolated silanol peak at 3744 cm^{-1}, which is either on the outer surface terminating the zeolite crystals or on silica impurities [17–19]. The intensity of this band is constant for all zeolites. SiOHAl groups, Brønsted-type acid sites, which were produced by hydrolysis of water at a cation or by deammoniation, gave rise to two IR absorption bands. The band at 3644 cm^{-1} (high-frequency (HF) band) was attributed to O–H groups within the large supercage. The low-frequency (LF) band at 3555 cm^{-1} appearing on H(13)CaY and H(26)CaY was assigned to hydroxyl groups hidden within the sodalite cages of the zeolite structure [19]. Furthermore, the O–H vibration at 3590 cm^{-1}, originating from $Ca(OH)_x$ species [10,13], decreased steeply and finally disappeared with increasing ammonia exchange level. The T–O–T overtone vibrations between 1700 and 1900 cm^{-1} showed a slightly red shift with increasing ammonia exchange level, in agreement with the literature [10,20].

Fig. 1b shows infrared spectra for activated Ca–NaY73 and Na–CaY71 samples with the same calcium content. A clear decrease in the band at 3644 cm^{-1} was observed for Na–CaY71 sample compared with both CaY and Ca–NaY73, which indicates that most of the protons were exchanged by sodium ions. Na–CaY71 and Ca–NaY73 showed similar intensities for the O–H vibration from isolated silanol (3744 cm^{-1}) and $Ca(OH)_x$ (3590 cm^{-1}) species.

The source of Brønsted acid sites of CaY zeolite is now generally accepted to occur during pretreatment or activation of a divalent cation-exchanged zeolite at elevated temperature via the reaction [10,15,17,18]

$$Ca^{2+} + H_2O(ad) + Si–O–Al \rightarrow Ca(OH)^+ + Si–O(H^+)–Al.$$

During the Na^+ back-exchange process, protons were replaced, based on the FTIR spectra and elemental analysis (Table 1):

$$Si–O(H^+)–Al + Na^+(solution) \rightarrow Si–O(Na^+)–Al + H^+(solution).$$

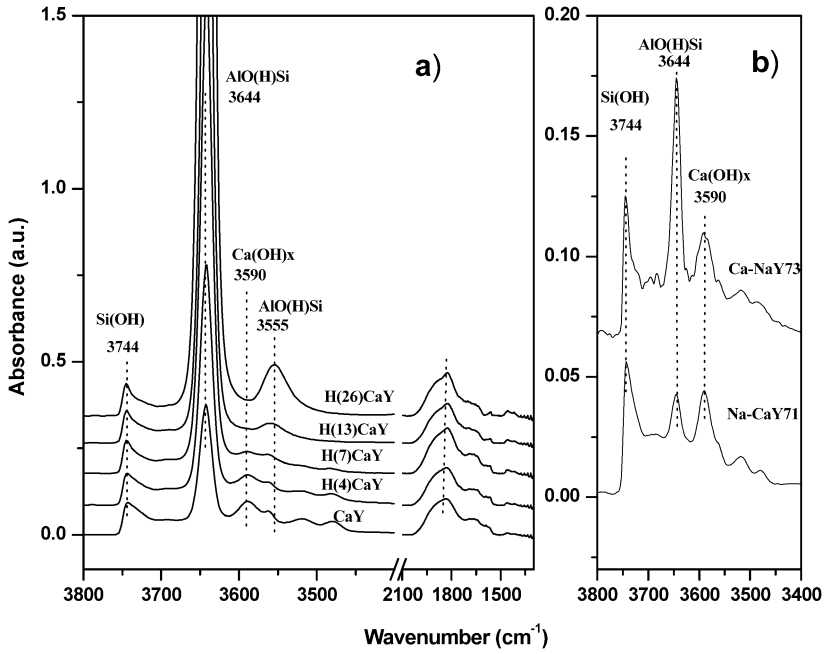

Fig. 1. Infrared spectra of (a) activated CaY and series HCaY zeolites; (b) activated Ca–NaY73 and Na–CaY71 zeolites.

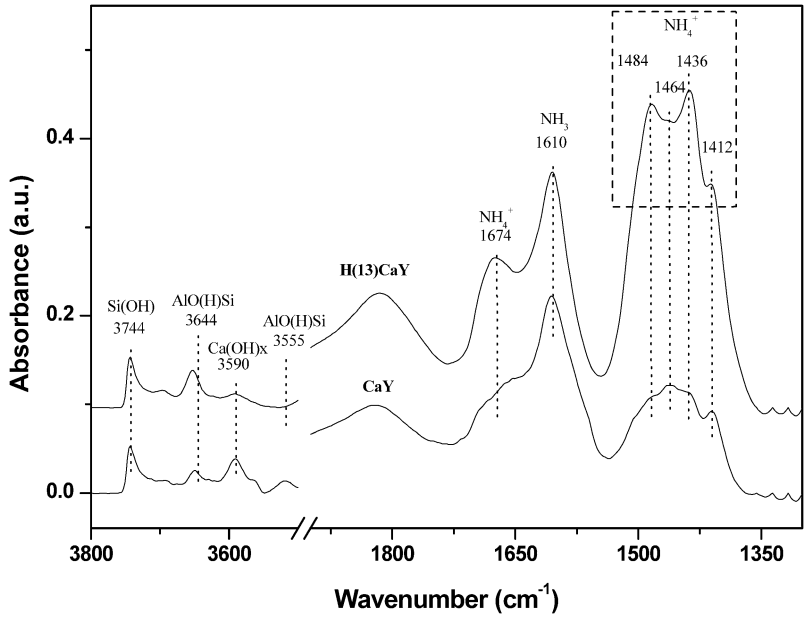

Fig. 2. Infrared spectra of ammonia adsorption on CaY and H(13)CaY zeolite.

Recently we showed that NH_3-TPD is a suitable technique for differentiating between the number and type of acid sites in calcium-exchanged Y zeolite samples [13]. Ammonia desorbing at low temperatures (between 150 and 300 °C, LT-NH_3) was identified as desorbing mainly from Brønsted acid sites, whereas desorption at higher temperatures (between 300 and 450 °C, HT-NH_3) was believed to originate from calcium cation sites in the zeolite supercage [13,21]. Comparison of the NH_3-TPD profiles of Ca–NaY73 and Na–CaY71 (not shown) confirmed a low amount of protons on Na–CaY71, whereas the amount of supercage Ca^{2+} ions was comparable to that observed for Ca–NaY73.

Furthermore, ammonia adsorption was studied with FTIR spectroscopy to differentiate between Lewis and Brønsted acid sites. Fig. 2 shows, as a typical example, the IR spectra for CaY and H(13)CaY after adsorption of 1 mbar NH_3 at 100 °C and subsequent evacuation (to remove physisorbed NH_3). Compared with the spectra in Fig. 1, the intensity of the hydroxyl stretch vibrations at 3644 and 3555 cm^{-1} clearly decreased. The hydroxyl groups at 3744

and 3590 cm^{-1} were not affected by ammonia adsorption, indicating a very weak acidity of silanol groups and $Ca(OH)_x$ species. Well-resolved absorbances appeared in the range of N–H deformation modes below 1700 cm^{-1}, which could be assigned to ammonia species adsorbed on different acid sites. The band at 1610 cm^{-1} was assigned to ammonia bound to Lewis sites [13,20–22]. Because no extra-framework aluminum was found by NMR for the studied samples, this species was attributed to ammonia coordinated to calcium cations. The bands at 1674 cm^{-1} and between 1484 and 1412 cm^{-1} were assigned to ammonium ions arising from the protonation of ammonia on Brønsted acid sites [13,20–22]. In agreement with previous results [13], all bands belonging to ammonium ions disappeared concurrently when the temperature was increased to 300 °C (not shown). A high number of Brønsted acid sites was observed on the H(13)CaY sample compared with CaY.

In conclusion, of the infrared spectra, ammonia adsorption and NH_3-TPD are in good agreement with the results of the zeolite chemical composition analysis (Table 1), and the expected changes in acidity were confirmed.

3.2. Propane adsorption

Fig. 3 displays the propane uptake at 1 mbar pressure (interpreted as the integrated FTIR band area between 3080 and 2660 cm^{-1}, details of spectra in Refs. [10,13]) by the different zeolites at room temperature. With increasing proton content, first (from CaY to H(7)CaY) a slight increase (15%) in propane uptake was found. However, from H(7)CaY to H(26)CaY, the propane amount decreased by about 50%. Interestingly, about 30% less propane was found on the Na–CaY71 zeolite (low Brønsted acidity) compared with Ca–NaY73 zeolite (high Brønsted acid sites).

Propane adsorption in alkaline-earth-exchanged Y zeolites has been reported to be due to enhanced interaction with framework oxygen and polarization at cation sites [10,13,23,24]. It has also been reported that propane could be adsorbed via hydrogen bonds to the Brønsted acid sites of acid Y zeolite [25]. To investigate the effect of Ca^{2+} cations and Brønsted acid sites on the propane adsorption capacity of these samples, ammonia adsorption was used to poison possible propane adsorption sites. It has been shown previously that at 100 °C ammonia adsorbs on both Ca^{2+} and Brønsted acid sites, whereas at 300 °C ammonia preferentially blocks Ca^{2+} cations [13].

Thus, one CaY sample was prepared by ammonia adsorption at 100 °C and subsequent evacuation (sample designated as CaY-100), and one was prepared by ammonia adsorption at 300 °C followed by evacuation (sample designated as CaY-300). Subsequently, both samples were cooled to room temperature, and 1 mbar propane was adsorbed. Fig. 4 shows infrared spectra for the hydroxyl vibration and C–H vibrations after these treatments in comparison with the adsorption of propane on untreated CaY. The infrared spectrum of the pretreated sample before exposure to propane was taken as a background. Three observations in particular are worth noting. First, CaY-100 infrared bands of propane at 2838 and 2887 cm^{-1}, present after propane adsorption on CaY, disappeared, whereas these two bands are still visible on CaY-300. Since the infrared band at 2838 and 2887 cm^{-1} appeared only when bare Ca^{2+} cations were present in the supercage [10,13], we concluded that these two bands originated from propane adsorbed on or close to supercage Ca^{2+} cations. Obviously, these sites are no longer accessible in CaY-100 and only partly available in CaY-300.

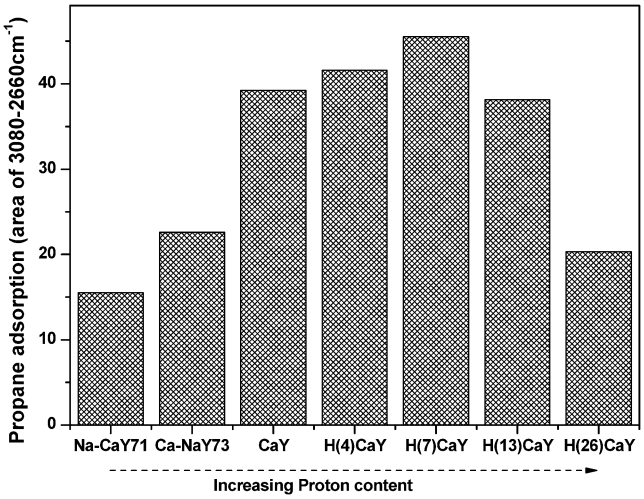

Fig. 3. Quantity of adsorbed propane at 1 mbar on Ca–NaY73, Na–CaY71 and series HCaY zeolites.

Second, compared with CaY, much less propane adsorbed (integrated area between 3080 and 2660 cm^{-1}) on CaY-300 (50%) and CaY-100 (10%). Third, no changes in the hydroxyl region could be observed for CaY-100 upon propane adsorption, which is in agreement with the fact that the pre-adsorbed ammonia blocks all of the Brønsted sites. For CaY-300 a decrease in the O–H band at 3640 cm^{-1} can be seen, but this is only about 10% of the original intensity of this band (Fig. 1). It has been reported that the contribution of Brønsted acid sites to the heat adsorption of propane is 6 kJ/mol compared with 31 kJ/mol for the total heat adsorption of propane adsorbed on HY zeolite [19,25]. Furthermore, the cation polarization of propane increases with increasing cation charge or decreasing cation radius. Adsorption of *n*-hexane on HY and NaY revealed as such a higher induction of polarity by protons than sodium cations [19,25]. The results of this study are in good agreement, since the quantity of adsorbed propane is increasing for Ca–NaY73 > Na–CaY71 (Fig. 3); they have the same calcium content, but there are fewer protons on Na–CaY71 compared with Ca–NaY73.

Comparing the polarization capability of Ca^{2+} and H^+ is more complicated, since from H^+ to Ca^{2+} both the charge (higher polarization) and cation radius (lower polarization) increase. Moreover, the mobility of H^+ in the zeolite also in-

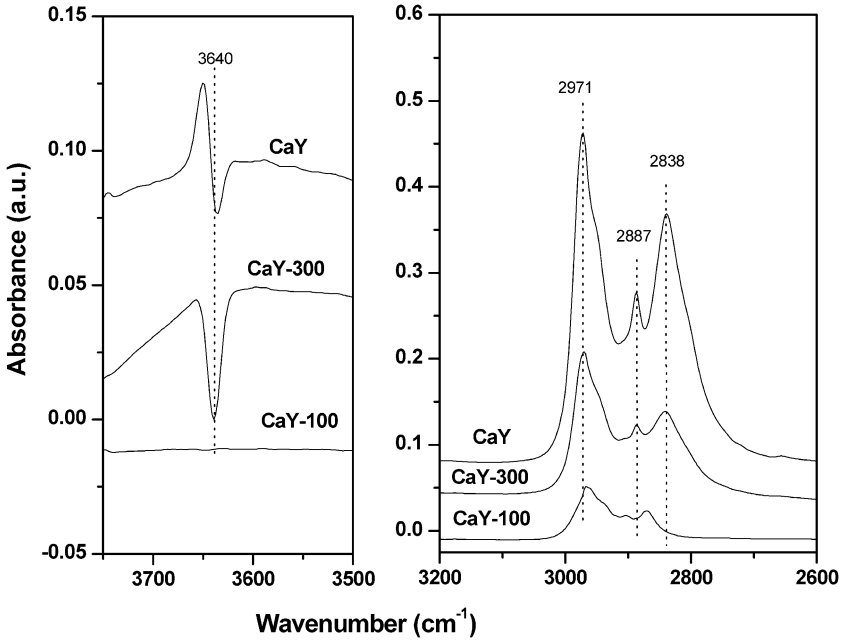

Fig. 4. Infrared spectra of 1 mbar propane adsorption on CaY with different pre-treatment conditions: CaY-100: adsorb NH_3 at 100 °C, followed by 5 h evacuation at 100 °C; CaY-300: adsorb NH_3 at 300 °C, followed by 1 h evacuation.

fluences the final effective electrostatic field. In addition, the FTIR data show that with increasing exchange of protons for calcium, the signal of the $Ca(OH)_x$ species (3590 cm^{-1}) diminished. The combination of this result with the Ca content (Table 1) indicates that first $Ca(OH)_x$ species are replaced by ammonium ions, followed by exchange of bare Ca^{2+} ions at higher proton exchange levels. As such the Ca content as determined by elemental analysis is gradually lowered with increased proton content. The change in amount of adsorbed propane (Fig. 3) can also be explained by the subsequent exchange of $Ca(OH)_x$ and Ca^{2+} ions. It was shown here (Fig. 4) and in previous studies that $Ca(OH)_x$ hardly contributes to the quantity of adsorbed propane [10]. A comparison of CaY to H(7)CaY shows that the Ca content decreased and the proton content increased, and simultaneously propane adsorption increased because of the affinity of propane for protons. A further decrease in the calcium content that occurs with proton exchange leads to removal of Ca^{2+} ions, which have a much higher propane affinity than protons, and consequently the amount of adsorbed propane drops significantly from H(7)CaY to H(26)CaY.

3.3. Propane oxidation: activity

Previously we showed that infrared spectroscopy is a suitable tool for the study of the selective propane oxidation at low pressures, with the goal of unraveling the reaction mechanism. The depletion of propane (between 3080 and 2660 cm^{-1}) and production of acetone (at 1682, 1421, 1379, and 1367 cm^{-1}) and water (infrared band at 3695 and 1634 cm^{-1}) were followed in the infrared spectra (details in Refs. [10,13]).

3.3.1. HCaY series

When 1 mbar of propane and 40 mbar of oxygen were loaded over the activated HCaY zeolites, a thermal reaction was noted at room temperature just minutes after introduction of the gases into the cell. All absorptions that were observed could be attributed to acetone and water [9,10,13].

Fig. 5a shows the acetone formation rate for the HCaY zeolites as a function of time, based on the amount of formation of adsorbed acetone. The same trends were observed for the consumption rate of adsorbed propane (interpreted as decreasing area of the infrared band between 3080 and 2660 cm^{-1}; not shown). CaY, H(4)CaY, and H(7)CaY showed a decreasing rate in time, whereas for H(13)CaY and H(26)CaY the rate first increased and after 10 h started to decrease. The highest initial acetone formation rate was observed for H(7)CaY, whereas H(13)CaY reached the same activity after about 10 h. Although the initial activities do not show a linear relationship with the amount of protons, it can be seen that after 10 h of reaction the deactivation rate steadily increased with higher proton amounts.

3.3.2. Ca–NaY73 and Na–CaY71

Room-temperature propane partial oxidation was further studied on Ca–NaY73 and Na–CaY71 zeolites, which contain the same calcium amount but have different Brønsted acidities. Fig. 5b reports the acetone formation rate as a function of reaction time; the activity of CaY was added as a reference. The initial acetone formation rate of Ca–NaY73 is approximately half that of CaY, whereas for Na–CaY71 the rate again was half of that of Ca–NaY73. Moreover, Ca–NaY73 showed a continuous decrease in the acetone formation rate, whereas Na–CaY71 showed a slight increase for the first 12 h of reaction.

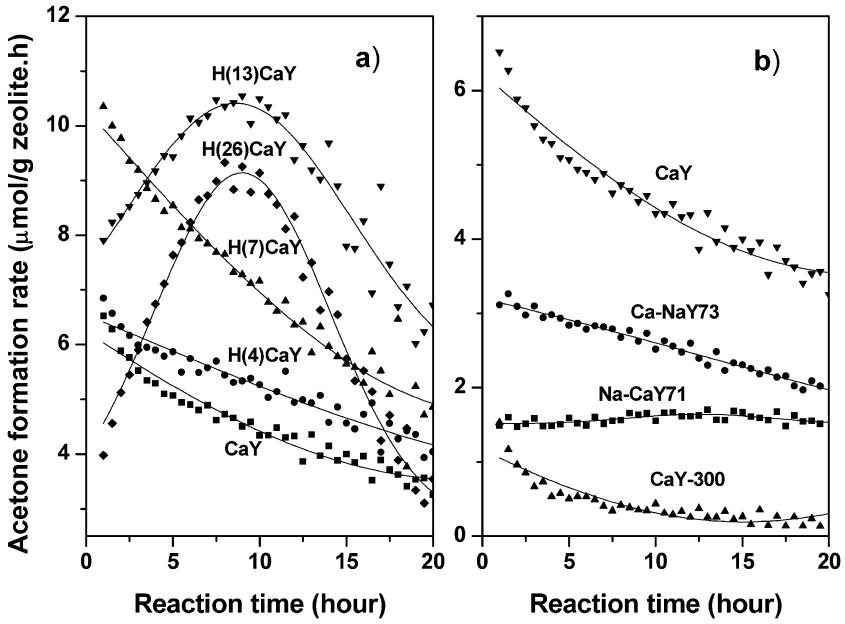

Fig. 5. Acetone formation rate as function of reaction time: (a) on CaY and series HCaY zeolite; (b) on Ca–NaY73, Na–CaY71, and CaY-300 (ammonia pre-adsorption at 300 °C).

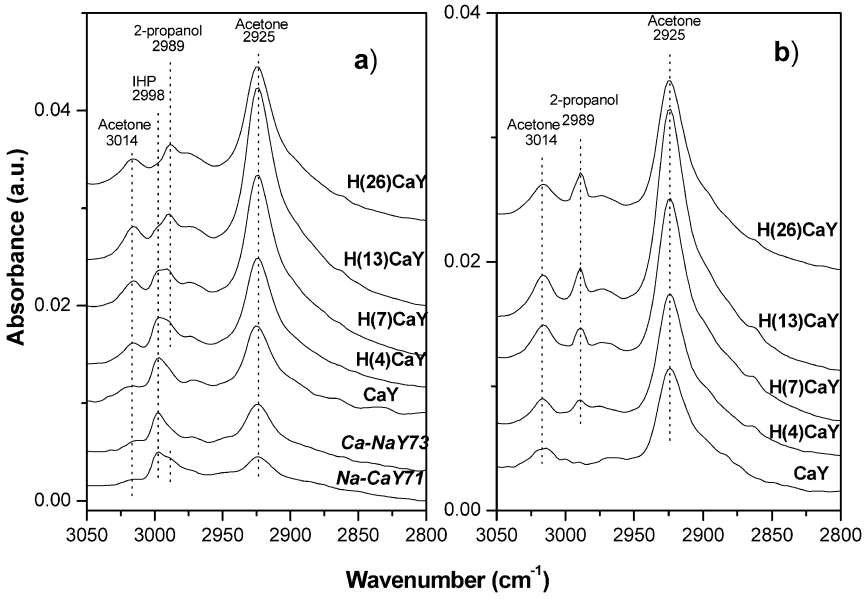

Fig. 6. IR spectra of (H)CaY zeolites (a) after 20 h reaction, followed by 5 min evacuation; (b) after heating of (a) at 200 °C 10 min and subsequent cooling to RT.

3.3.3. Ammonia-pretreated samples

After 1 mbar and 40 mbar oxygen were loaded into the ammonia-pretreated zeolites, the formation of acetone and water was followed (Fig. 5b). CaY-100 did not show any activity at room temperature (not shown), whereas CaY-300 exhibited an activity that was one-tenth that of the untreated CaY zeolite. Clearly, in addition to the propane adsorption capacity, the presence of supercage Ca^{2+} ions is also essential for the selective oxidation of propane, as these Ca^{2+} supercage ions are selectively occupied with NH_3 at 300 °C, as discussed before.

3.4. Propane oxidation: selectivity

To investigate the selectivity of the reaction, adsorbed propane was removed by 5 min of evacuation after 20 h of reaction (Fig. 6a). Only propane was detected by on-line MS analysis during evacuation. Bands at 3014, 2998, 2989, and 2925 cm^{-1} were observed that were initially masked by propane. These bands could be attributed to isopropylhydroperoxide (IHP) (2998 cm^{-1}) and acetone (3014 and 2925 cm^{-1}) [10,12,13], and the band at 2989 cm^{-1} was assigned to 2-propanol, as confirmed by comparison with

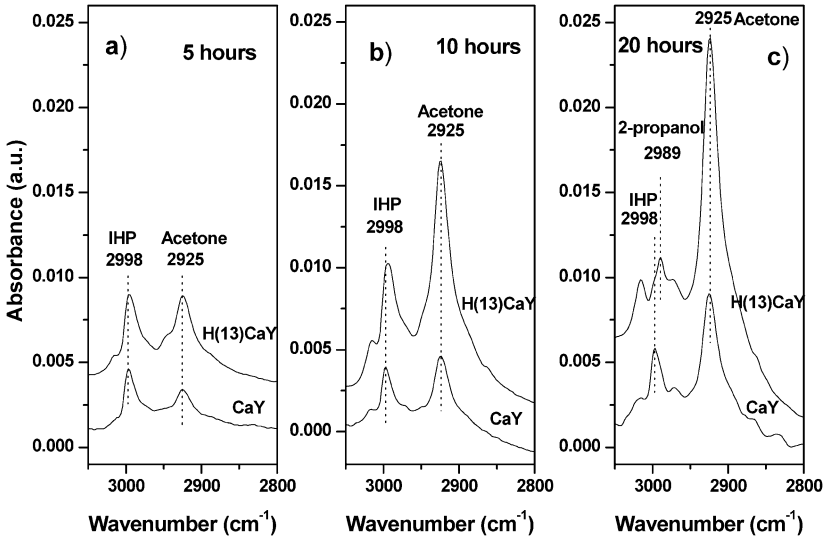

Fig. 7. Infrared spectra after reaction of 1 mbar propane and 40 mbar propane on CaY and H(13)CaY: (a) 5 h, followed by 5 min evacuation; (b) 10 h, followed by 5 min evacuation; (c) 20 h, followed by 5 min evacuation.

the IR spectrum after adsorption of 2-propanol in CaY. The O–H stretch vibration of 2-propanol could not be observed because it overlaps with the water O–H stretch vibrations. Complete selectivity for acetone was observed on CaY, in agreement with previous results [10,12,13]. However, acetone selectivity decreased for the proton-exchanged zeolites since 2-propanol was formed. Furthermore, the IHP amount decreased with increasing Brønsted acidity. Surprisingly, for Na–CaY71, which has a low number of protons, large quantities of IHP and 2-propanol were observed (Fig. 6a, bottom line). Furthermore, a higher molar ratio of IHP to acetone was found for Na–CaY71 compared with Ca–NaY73.

Previously it was shown that at 200 °C IHP can easily be decomposed into acetone and water without desorption of acetone [12]. Thus, the system was further heated to 200 °C (10 °C/min), kept at 200 °C for 10 min, and cooled to room temperature, after which FTIR spectra were taken (Fig. 6b). Clearly, the band at 2998 cm^{-1} (IHP) disappeared, with a concurrent growth of the acetone C=O band, whereas the band at 2989 cm^{-1} (2-propanol) still showed on the spectra. Except for water, no desorption of other product molecules were detected by infrared spectroscopy and on-line MS analysis during IHP conversion.

To better understand 2-propanol and acetone formation, two typical samples (CaY and H(13)CaY) were selected for the investigation of selectivity at different reaction times (Fig. 7). The amounts of IHP and acetone formed at different reaction times are listed in Table 2. For CaY, the IHP concentration decreased slightly from 5 to 20 h of reaction, whereas for H(13)CaY, the IHP concentration increased from 5 to 10 h of reaction and dramatically decreased after 20 h of reaction. Furthermore, the concentrations of both IHP and acetone were higher for H(13)CaY compared with CaY at both 5 h and 10 h of reaction, whereas a lower IHP concentration for H(13)CaY was found after 20 h of reaction compared with CaY. In addition, after decomposition of

Table 2
IHP and acetone concentration at different reaction time during selective propane oxidation

Time (h)	CaY		H(13)CaY	
	IHP (μmol/g)	Acetone (μmol/g)	IHP (μmol/g)	Acetone (μmol/g)
5	6.7	30	7.7	46
10	6.0	53	14.9	97
20	6.0	92	3.6	178

IHP, acetone and water were formed exclusively on CaY and H(13)CaY after 5 h, whereas small amounts of 2-propanol (band at 2989 cm^{-1}) were also observed on H(13)CaY after 10 and 20 h of reaction. For H(13)CaY a significant higher amount of 2-propanol was observed for 20 h of reaction compared with 10 h of reaction.

It has been proposed that a possible reaction path for the production of alcohol is the reaction between a hydroperoxide and a hydrocarbon to form two molecules of alcohol [7]. To test this suggested reaction path, two parallel experiments were carried out. Since IHP cannot be loaded into the zeolites, first 5 h of reaction was performed for two batches of CaY with 1 mbar of propane and 40 mbar of oxygen, followed by 5 min of evacuation. In the first experiment, the system was continuously evacuated for 7 h. In the second experiment, 1 mbar of propane was reloaded and kept for 7 h, followed by 5 min of evacuation. The infrared spectra obtained after those two treatments are given in Fig. 8.

Decomposition of IHP leads to acetone and water only (Fig. 8a, experiment 1). Some IHP was left after 7 h since the reaction was done at room temperature. In the presence of propane, however, 2-propanol was produced in addition to acetone and water (Fig. 8b, experiment 2). Moreover, less acetone was produced, indicating that part of the IHP converted into 2-propanol instead of acetone and water.

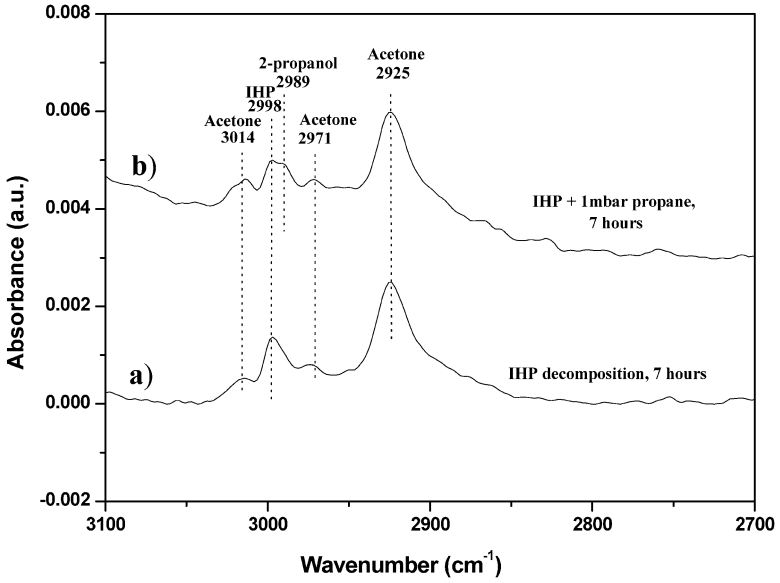

Fig. 8. Infrared spectra after 5 h reaction of 1 mbar propane and 40 mbar oxygen on CaY at room temperature (a) followed by 7 h evacuation; (b) followed by 5 min evacuation, subsequent loading of 1mbar propane and dwell of 7 h, followed by 5 min evacuation.

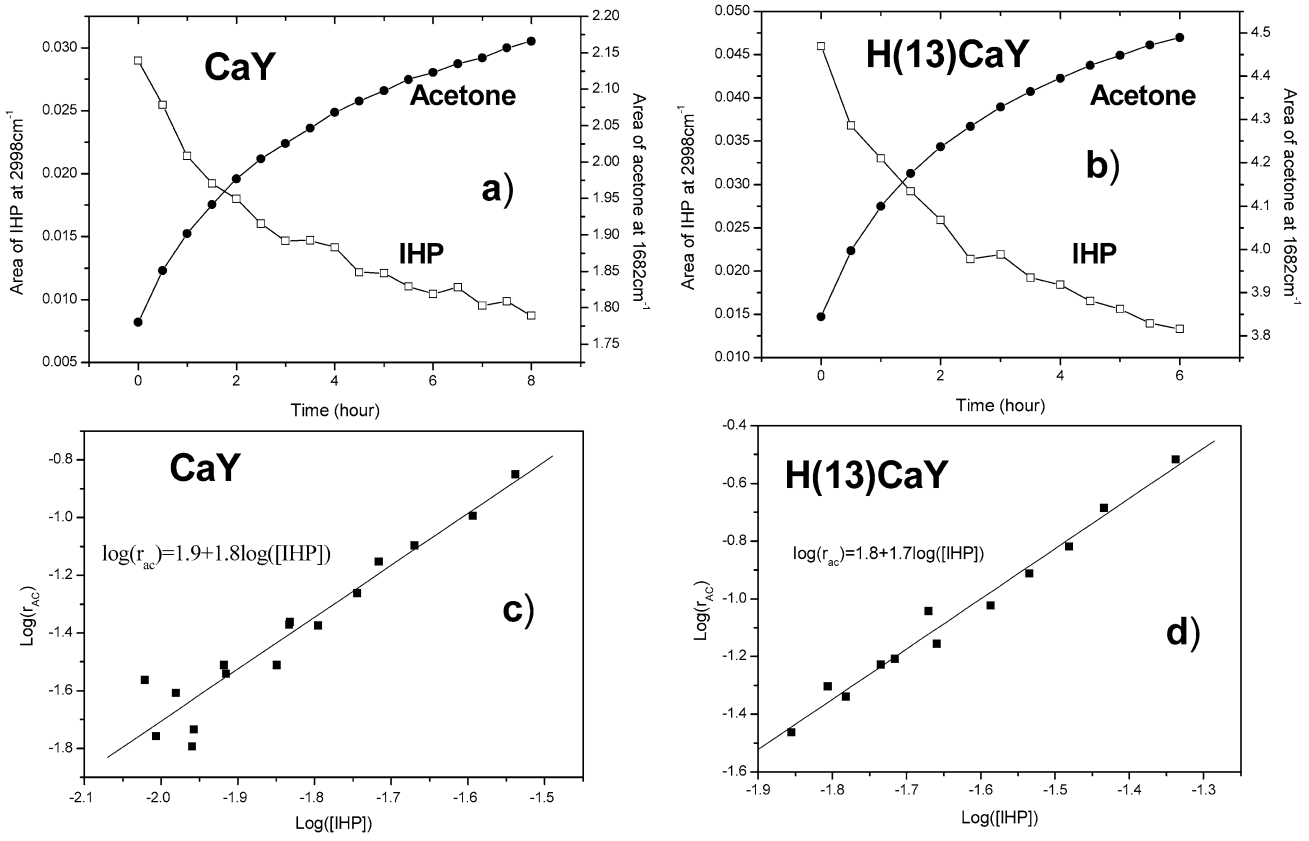

Fig. 9. Acetone and IHP concentration as function of time during IHP decomposition at room temperature (a) on CaY zeolite; (b) on H(13)CaY zeolite. Kinetic analysis of room temperature IHP decomposition on (c) CaY zeolite; (d) H(13)CaY zeolite.

3.5. Kinetics of IHP decomposition

Finally, the kinetics of IHP decomposition in the absence of propane was studied. For CaY and H(13)CaY, after 5 h of reaction at room temperature with 1 mbar of propane and 40 mbar of oxygen, the system was evacuated. Subsequently, IHP decomposition and acetone formation were monitored by infrared spectroscopy at room temperature (Figs. 9a and 9b). For both samples a decrease in IHP and a concurrent increase in acetone were observed. On-line mass

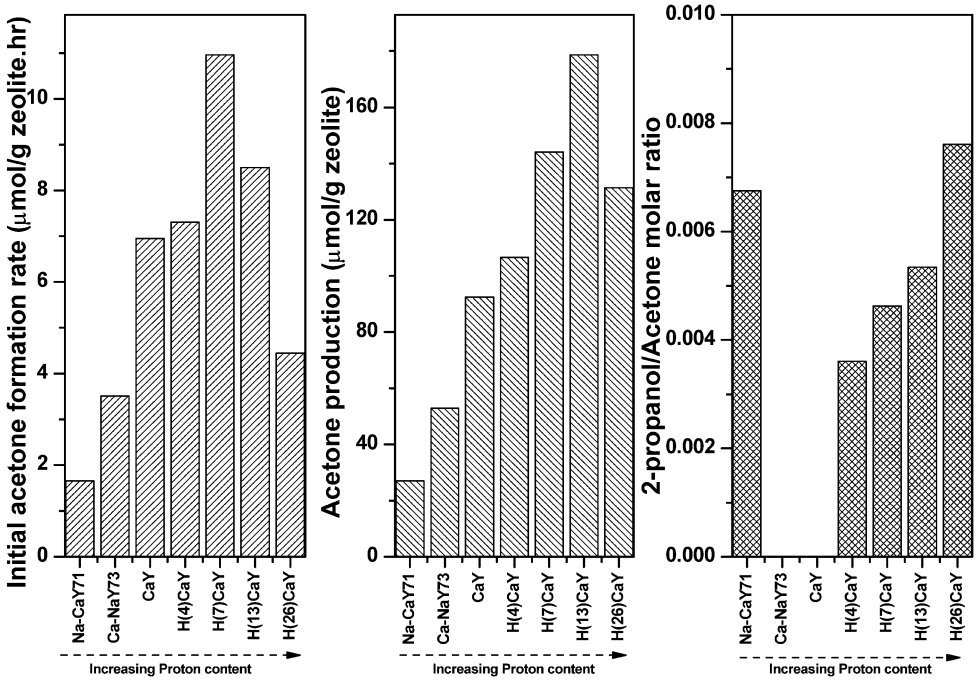

Fig. 10. (a) Initial acetone formation rate; (b) acetone formation after 20 h reaction; (c) 2-propanol to acetone ratio on (Na)(H)CaY zeolites.

spectroscopy revealed no products in the gas phase. From the results in Figs. 9a and 9b, the rate of IHP decomposition into acetone was analyzed (Figs. 9c and 9d). Clearly, plotting log[r_{AC}] versus log[IHP] ([r_{AC}]: rate of acetone formation, area(band at 1682 cm^{-1})/h; [IHP]: area(band at 2998 cm^{-1})) results in a straight line from which the order in IHP was determined: 1.8 and 1.7 for CaY and H(13)CaY, respectively.

3.6. General discussion

This study shows that with an increasing of number of protons in the series Na–CaY71 > Ca–NaY73 > CaY > H(4)CaY > H(7)CaY > H(13)CaY > H(26)CaY, Volcano-type plots are observed for

- amount of adsorbed propane (Fig. 3),
- initial acetone formation rate (Fig. 10a),
- total amount of acetone produced after 20 h of reaction (Fig. 10b),
- acetone selectivity (Fig. 10c).

Interestingly, the maximum of the Volcano plots for amount of adsorbed propane, initial acetone activity, and total amount of acetone produced varies between H(7)CaY and H(13)CaY. Fig. 11 shows initial acetone formation rates as a function of propane adsorption. Although, in general, a linear trend is observed between the amount of adsorbed propane and the initial acetone formation rate, the scattering of the points is beyond the experimental error. Therefore, the amount of adsorbed propane cannot fully account for

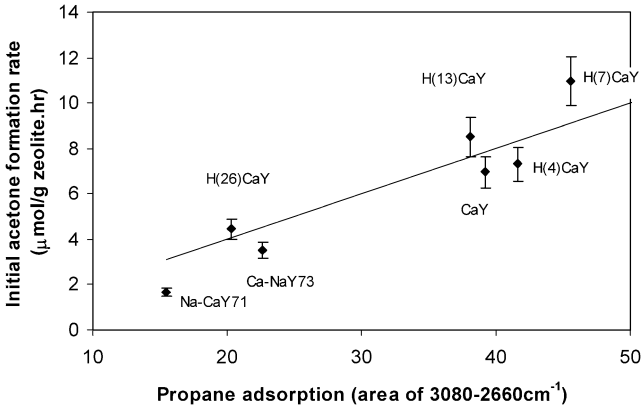

Fig. 11. Initial acetone formation rate as a function of amount of adsorbed propane on (Na)(H)CaY zeolites.

the observed differences in activity as a function of catalyst composition.

At present, in the literature it is proposed that the active site for the activation of propane in this reaction is a bare Ca^{2+} cation, located in the supercage [13]. The electrostatic field of the cation is thought to be capable of stabilizing charge-transfer states between propane and oxygen [$C_3H_8{}^+O_2{}^-$] by Coulombic interaction [9–11,26]. Subsequent abstraction of a proton from the acidic hydrocarbon cation to the basic superoxygen ion should result in the formation of $C_3H_7{}^*$ and $HO_2{}^*$ radicals. Recombination of these radicals into IHP is possible, or, at elevated temperature, they may start a radical chain reaction. However, in the restricted zeolite cages and at relatively low temperature, the radical recombination reaction is faster than the radical chain reaction [26]. Finally, it was shown that if a ze-

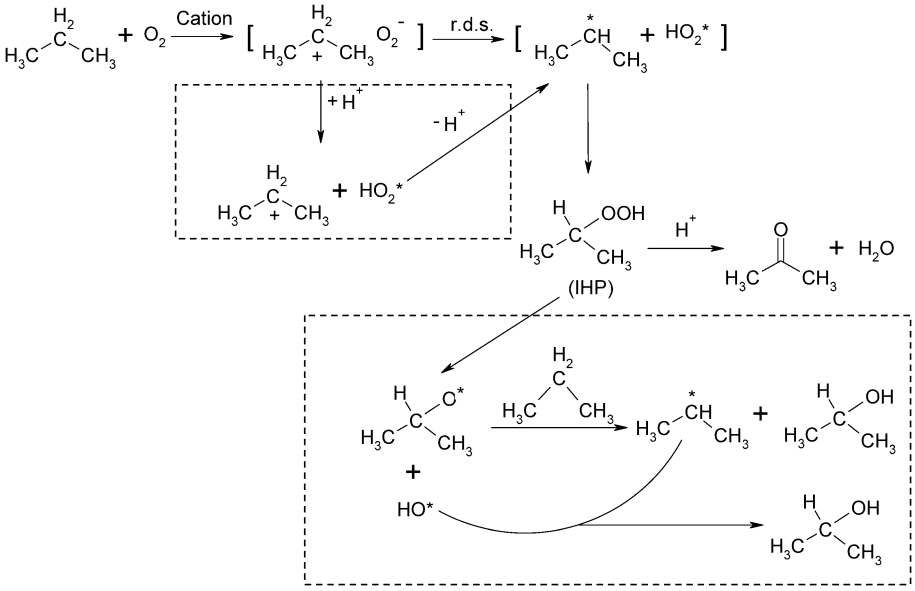

Scheme 1. Proposed mechanism for propane oxidation over proton modified CaY zeolite. The reactions in the dashed boxes are based on the findings in the present paper. The other reactions in the scheme have been discussed before in literature [9–11,13,26].

olite contains Brønsted acid sites in addition to earth-alkali cations, IHP can be decomposed into acetone and water [10]. Scheme 1 summarizes these reactions. In the following discussion we will extend this mechanism with additional reactions (dashed boxes in Scheme 1) based on the present findings.

3.6.1. Catalytic effect of protons on IHP formation

The importance of supercage Ca^{2+} cations for propane oxidation reaction, as reported earlier [13], was confirmed in this study by propane adsorption and oxidation after pre-adsorption of ammonia (Fig. 4). Blocking of all supercage Ca^{2+} cations and Brønsted acid sites by adsorbed ammonia caused a significant change in propane adsorption and a total inhibition of oxidation activity (Fig. 4). When part of the ammonia was released from calcium cation sites and all Brønsted acid sites were recovered (CaY-300), a large decrease in propane oxidation activity was found compared with CaY without pre-adsorption of ammonia (Fig. 5b). However, the data on the concentrations of IHP and acetone in CaY and H(13)CaY after 5 and 10 h (Fig. 7, Table 2) contradict the conclusion obtained with the model that Ca^{2+} ions are exclusively responsible for the formation of IHP. Although less propane adsorption was observed on H(13)CaY (Fig. 3), and H(13)CaY contains only about 70% of the number of supercage Ca^{2+} ions as compared with CaY (Table 1), after 5 h of reaction the amount of IHP formed on H(13)CaY is already 1.1 times higher than that found for CaY, wheres after 10 h it is about 2.5 times higher than for CaY (Table 2). In addition, more acetone was produced on H(13)CaY compared with CaY for both 5 and 10 h of reaction.

As stated above, the critical point of formation of IHP is thought to be a charge-transfer complex $[C_3H_8{}^+O_2{}^-]$, followed by the rate-determining step of proton abstraction from the acidic hydrocarbon cation ($C_3H_8{}^+$) to basic superoxygen ($O_2{}^-$), to form $C_3H_7{}^*$ and $HO_2{}^*$ radicals, which then rapidly recombine into IHP (1). The observed influence of protons on the enhancement of IHP formation can be explained by a catalytic effect of the protons of the zeolite in the proton-abstraction step:

$$[C_3H_8{}^+O_2{}^-] + H^+ \rightarrow C_3H_8{}^+ + HO_2{}^*, \quad (2)$$

$$C_3H_8{}^+ \rightarrow C_3H_7{}^* + H^+, \quad (3)$$

$$C_3H_7{}^* + HO_2{}^* \rightarrow C_3H_7OOH\ (IHP). \quad (4)$$

Since the proton abstraction of the charge-transfer complex was found to be rate determining [7], the catalytic effect of protons on the IHP formation rate can be explained by the opening of an alternative, faster route to IHP via reactions (2) to (4).

This would indeed result in a Volcano type of behavior as a function of proton content, since with increasing $[H^+]$ the amount of supercage Ca^{2+} concurrently decreased (Table 1) and thus the amount of formed charge-transfer complexes decreased. The combination of these two phenomena leads to an optimum for Ca^{2+} and H^+ concentration on the oxidation activity, as was observed (Fig. 10).

For HCaY13 and HCaY26 a significant increase in acetone formation rate was observed in the first 10 h of reaction, whereas the other zeolites showed only a deactivation as a function of time. Again, two phenomena take place at the same time. First, the amount of IHP increases with higher proton content according to the reactions (2) to (4), as discussed above. Since the conversion of IHP into acetone is a second-order reaction (Fig. 9), higher IHP concentrations will increase the acetone formation rate because the IHP concentration increases in time (Table 2). In particular, for H(13)CaY and H(26)CaY the very high Brønsted acidity in

the samples (Fig. 1) will strongly enhance the catalytic pathway from (2) to (4), resulting in increased amount of IHP in the first 10 h, as observed in Fig. 7. The observation also strongly implied that with increasing proton concentration, the rates of proton abstraction and IHP decomposition are becoming competitive. At the same time, the production of acetone and water deactivates the samples since the product molecules remain adsorbed on the active cations and protons [10]. The formation rate of the charge-transfer complex would decrease faster when more water is produced and fewer supercage Ca^{2+} ions are present. This indeed agrees with the increasing deactivation rate with increasing proton content and decreasing Ca^{2+} amount (Fig. 5).

3.6.2. 2-Propanol production

Similar to the activity, the selectivity for acetone shows a Volcano type of behavior as a function of H^+/Ca^{2+} ratio (Fig. 10c). However, in this case the optimum selectivity is found at much lower proton content, namely for CaNaY73 and CaY (100%). With both increasing and decreasing Brønsted acidity, 2-propanol was found as a by-product. Inspired by the work of Vanoppen et al. for liquid-phase oxidation of cyclohexane [16], it may be suggested that ion-exchanged Y zeolites are also capable of catalyzing homolytic IHP decomposition. Fig. 8 showed that the addition of propane to IHP in the absence of oxygen on CaY led to the formation of propanol. Since infrared spectra have revealed that adsorbed IHP adsorbed close to the cation sites [10], the calcium cation could activate the peroxide bond in IHP, which results in the formation of $C_3H_7O^*$ and HO^* radicals. Subsequently, an alkyloxyl radical reacts with propane, followed by radical recombination into two molecules of 2-propanol:

$$C_3H_7OOH \rightarrow C_3H_7O^* + HO^*, \quad (5)$$

$$C_3H_7O^* + C_3H_8 \rightarrow C_3H_7OH + C_3H_7{}^*, \quad (6)$$

$$C_3H_7{}^* + HO^* \rightarrow C_3H_7OH. \quad (7)$$

The contribution of reactions (5)–(7) demonstrate that the zeolite cages cannot be considered to be completely isolated, as propane added later is involved. Because only small amounts of 2-propanol were found throughout the series, reactions (5)–(7) must be slower than the decomposition of IHP into acetone and water. Decreasing Brønsted acid sites slow down IHP decomposition into acetone and water, thus favoring the competing route via IHP homolytic cleavage, which explains the increased 2-propanol formation, as was found for Na–CaY71. In addition, for H(13)CaY much more 2-propanol was formed after 20 h than after 10 h of reaction (Fig. 7), whereas the concentration of IHP (Table 2) and the acetone formation rate (Fig. 5) dramatically decreased in this time span. Again, IHP decomposition into acetone is slowed down, which favors the homolytic splitting, resulting in 2-propanol. As such, the balance between IHP catalytic decomposition into acetone and IHP homolysis to produce 2-propanol is influenced by the H^+/Ca^{2+} ratio of the sample. Although the reaction in this study was carried out at very low pressure, no other reaction pathways have been observed at atmospheric pressure and room temperature [9,10].

4. Conclusions

The importance of Brønsted acid sites for propane partial oxidation to acetone in CaY was investigated by in situ FTIR spectroscopy. With increasing concentration of Brønsted acid sites on calcium-exchanged Y zeolite, Volcano-type plots were observed for (1) the amount of adsorbed propane; (2) the initial acetone formation rate; (3) the total amount of acetone produced after 20 h of reaction; (4) acetone selectivity. The results clearly show that Brønsted acidity increases the IHP formation rate, most likely via a catalytic H^+ abstraction and the IHP decomposition into acetone and water. Formation of a minor amount of 2-propanol was observed when the Brønsted acidity was decreased or increased compared with the fully Ca-exchanged sample. This was attributed to a parallel reaction pathway of IHP homolytic decomposition in addition to IHP decomposition into acetone and water. This study convincingly shows that the activity and selectivity of Ca-exchanged Y-zeolites are determined by a subtle balance between the number of supercage Ca^{2+} ions and Brønsted acid sites.

Acknowledgments

This work was performed under the auspices of the Dutch Institute for Research in Catalysis (NIOK). We thank J.A.M. Vrielink for the XRF measurements and Bert Geerdink for technical support. The financial support from CW/STW (Project no. 790-36-057) is gratefully acknowledged.

References

[1] G. Centi, F. Cavani, F. Trifiro, Selective Oxidation by Heterogeneous Catalysis, Kluwer Academic/Plenum, New York, 2000.
[2] M. Ai, Catal. Today 42 (1998) 297.
[3] J.S. Clarke, J.H. Kroll, N.M. Donahue, J.G. Anderson, J. Phys. Chem. A 102 (1998) 9847.
[4] L. Luo, J.A. Labinger, M.E. Davis, J. Catal. 200 (2001) 222.
[5] G. Centi, F. Trifiro, Appl. Catal. A 143 (1996) 3.
[6] F. Blatter, H. Sun, H. Frei, Chem.-Eur. J. 2 (1996) 385.
[7] R.G. Larsen, A.C. Saladino, T.A. Hunt, J.E. Mann, M. Xu, V.H. Grassian, S.C. Larsen, J. Catal. 204 (2001) 440.
[8] H. Sun, F. Blatter, H. Frei, J. Am. Chem. Soc. 118 (1996) 6873.
[9] H. Sun, F. Blatter, H. Frei, Catal. Lett. 44 (1997) 247.
[10] J. Xu, B.L. Mojet, J.G. van Ommen, L. Lefferts, Phys. Chem. Chem. Phys. 5 (2003) 4407.
[11] D.L. Vanoppen, D.E. De Vos, P.A. Jacobs, Progr. Zeolite Micropor. Mater. A–C 105 (1997) 1045.
[12] J. Xu, B.L. Mojet, J.G. van Ommen, L. Lefferts, J. Phys. Chem. B 108 (2004) 218.

[13] J. Xu, B.L. Mojet, J.G. van Ommen, L. Lefferts, J. Phys. Chem. B 108 (2004) 15728.
[14] A.G. Panov, R.G. Larsen, N.I. Totah, S.C. Larsen, V.H. Grassian, J. Phys. Chem. B 104 (2000) 5706.
[15] Y. Xiang, S.C. Larsen, V.H. Grassian, J. Am. Chem. Soc. 121 (1999) 5063.
[16] D.L. Vanoppen, D.E. De Vos, P.A. Jacobs, J. Catal. 177 (1998) 22.
[17] J.W. Ward, J. Phys. Chem. 72 (1968) 4211.
[18] J.W. Ward, J. Catal. 10 (1968) 34.
[19] D.W. Breck, Zeolite Molecular Sieves: Structure, Chemistry, and Use, Wiley, New York, 1974.
[20] J.E. Sponer, Z. Sobalik, J. Phys. Chem. B 105 (2001) 8285.
[21] H. Miessner, H. Kosslick, U. Lohse, B. Parlitz, V.-A. Tuan, J. Phys. Chem. 97 (1993) 9741.
[22] K. Nakamoto, Infrared Spectra of Inorganic and Coordination Compounds, Wiley–Interscience, New York, 1986.
[23] H. van Bekkum, E.M. Flanigen, P.A. Jacobs, J.C. Jansen, Introduction to Zeolite Science and Practice, Elsevier, Amsterdam, 2001.
[24] B. Smit, J. Phys. Chem. 99 (1995) 5597.
[25] F. Eder, Thermodynamics and Siting of Alkane Sorption in Molecular Sieves, Ph.D. Thesis, University of Twente, Enschede, 1996.
[26] F. Blatter, H. Sun, S. Vasenkov, H. Frei, Catal. Today 41 (1998) 297.